Numerical simulation of the three-dimensional river antidunes

Toshiki IWASAKI (Hokkaido University), Takuya INOUE, and Hiroki YABE (Civil Engineering Research Institute for Cold Regions, Sapporo, Japan) Shinichiro ONDA (Kyoto Univeristy, Japan)

Introduction

Understanding the dynamics of bedforms in rivers is of great importance from the engineering point of view. In steep rivers, the flow becomes supercritical during a flood, resulting in formation of antidunes on the bed. The antidunes have sometimes important role in developing a triangle-shape water surface wave (standing wave) as shown in Figure 1. Since this surface wave may be a potential risk for the river management works, it is important to predict the dynamics of this kind of waves and bedforms.

The water surface wave shown above has a strong three-dimensional shape, so that the antidunes formed on the bed may be also three dimensional. However, there is a lack of understanding the formation and development of three-dimensional antidunes. We proposed a model framework to capture the formation of three-dimensional antidunes (Iwasaki et al., 2016). The linear stability analysis shows that the proposed model is in part able to reproduce the three-dimensional river antidunes (Figure 2). In this study, we perform numerical simulations to understand the model performance at the nonlinear level.

Figure 1. A triangle-shape water surface wave observed during a flood in Toyohira River, Japan.

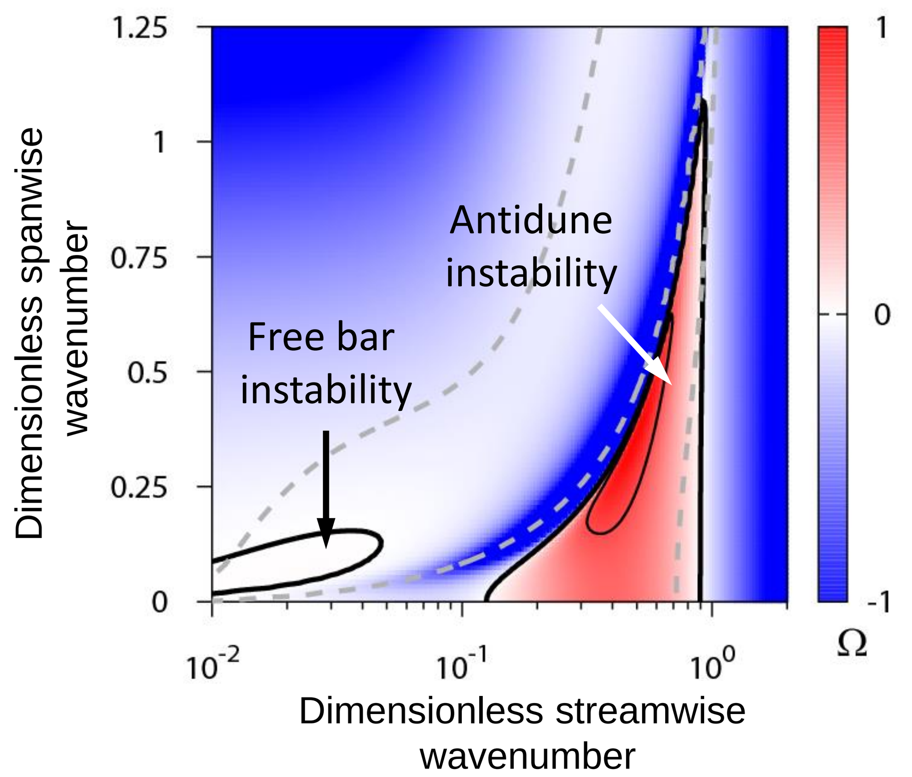

Figure 2. The instability diagrams of 3D antidunes. The parameters are Fr=1.25, τ_{*0}=0.16, C_f=10.6^{-2}.

Model

Flow model: Boussinesq model

$$\frac{\partial h}{\partial t}+\frac{\partial Uh}{\partial x}+\frac{\partial Vh}{\partial y}=0$$

$$\frac{\partial U}{\partial t}+U\frac{\partial U}{\partial x}+V\frac{\partial U}{\partial y}=g\sin\theta-g\left(\frac{\partial h}{\partial x}+\frac{\partial \eta}{\partial x}\right)-\frac{1}{h}\frac{\partial}{\partial x}\int_\eta^H\frac{p}{\rho}dz-\frac{\tau_x}{\rho h}$$

$$\frac{\partial V}{\partial t}+U\frac{\partial V}{\partial x}+V\frac{\partial V}{\partial y}=-g\left(\frac{\partial h}{\partial y}+\frac{\partial \eta}{\partial y}\right)-\frac{1}{h}\frac{\partial}{\partial y}\int_\eta^H\frac{p}{\rho}dz-\frac{\tau_y}{\rho h}$$

$$\int_\eta^H\frac{p}{\rho}dz=-h^3\left(B+\frac{1}{3}\right)\left(\frac{\partial}{\partial x}\frac{\partial U}{\partial t}+\frac{\partial}{\partial y}\frac{\partial V}{\partial t}\right)-\frac{h^3}{3}\left[U\left(\frac{\partial^2 U}{\partial x^2}+\frac{\partial^2 V}{\partial x\partial y}\right)+V\left(\frac{\partial^2 U}{\partial x\partial y}+\frac{\partial^2 V}{\partial y^2}\right)\right]$$
$$+\frac{h^2}{2}\left(U^2\frac{\partial^2\eta}{\partial x^2}+2UV\frac{\partial^2\eta}{\partial x\partial y}+V^2\frac{\partial^2\eta}{\partial y^2}\right)-\frac{h^3}{3}Bg\left(\frac{\partial^2 H}{\partial x^2}+\frac{\partial^2 H}{\partial y^2}\right)$$

$$V_b=\sqrt{{u_b}^2+{v_b}^2}$$

$$u_b=U-h\left[\frac{1}{2}\left(\frac{\partial U}{\partial x}\frac{\partial\eta}{\partial x}+U\frac{\partial^2\eta}{\partial x^2}+\frac{\partial V}{\partial x}\frac{\partial\eta}{\partial y}+V\frac{\partial^2\eta}{\partial x\partial y}\right)+\frac{1}{6}\left(\frac{\partial U}{\partial x}\frac{\partial h}{\partial x}+U\frac{\partial^2 h}{\partial x^2}+\frac{\partial V}{\partial x}\frac{\partial h}{\partial y}+V\frac{\partial^2 h}{\partial x\partial y}\right)\right]$$

$$v_b=V-h\left[\frac{1}{2}\left(\frac{\partial U}{\partial y}\frac{\partial\eta}{\partial x}+U\frac{\partial^2\eta}{\partial x\partial y}+\frac{\partial V}{\partial y}\frac{\partial\eta}{\partial y}+V\frac{\partial^2\eta}{\partial y^2}\right)+\frac{1}{6}\left(\frac{\partial U}{\partial y}\frac{\partial h}{\partial x}+U\frac{\partial^2 h}{\partial x\partial y}+\frac{\partial V}{\partial y}\frac{\partial h}{\partial y}+V\frac{\partial^2 h}{\partial y^2}\right)\right]$$

Non-equilibrium bedload transport model

$$\frac{\partial q_{bx}}{\partial t}+\frac{\partial u_{px}q_{bx}}{\partial x}+\frac{\partial u_{py}q_{bx}}{\partial y}=\frac{1}{l_s}\left(u_{pxe}q_{be}-u_{px}q_b\right)$$

$$\frac{\partial q_{by}}{\partial t}+\frac{\partial u_{px}q_{by}}{\partial x}+\frac{\partial u_{py}q_{by}}{\partial y}=\frac{1}{l_s}\left(u_{pye}q_{be}-u_{py}q_b\right)$$

$$q_{be}=4\left(\tau_*-\tau_{*c}\right)^{3/2}\sqrt{S_g g d^3}$$

$$\left(u_{px},u_{py},u_{pxe},u_{pye}\right)=\frac{1}{L_a(1-\lambda)}\left(q_{bx},q_{by},q_{bxe},q_{bye}\right)$$

$$q_{bex}=\frac{u}{V}q_{be}-\frac{v}{V}q_{ben},\quad q_{bey}=\frac{v}{V}q_{be}+\frac{u}{V}q_{ben}$$

$$q_{ben}=q_{be}\left(\frac{u_{bn}}{V_b}-\sqrt{\frac{\tau_{*c}}{\mu_s\mu_k\tau_*}}\frac{\partial\eta}{\partial n}\right)$$

$$(1-\lambda)\frac{\partial\eta}{\partial t}+\frac{\partial q_{bx}}{\partial x}+\frac{\partial q_{by}}{\partial y}=0$$

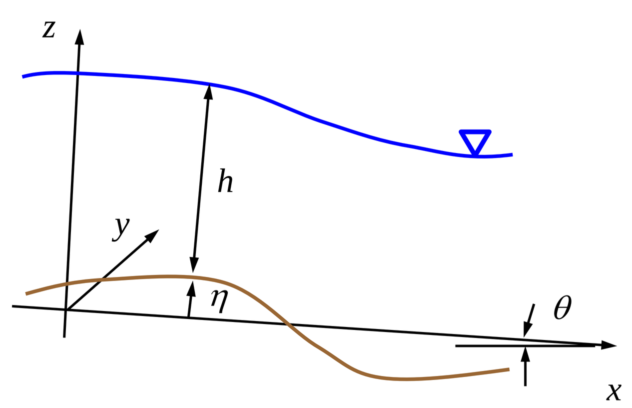

Figure 3. The coordinate system.

Notations: t is the time, x, y, z are the streamwise, spanwise and vertical coordinate, U, V are the depth-averaged flow velocity in x, y directions, h is the water depth, η is the deviation from the average bed elevation, θ is the longitudinal angle of average bed elevation, H is the water level, p is the pressure, τ_x, τ_y are the bed shear stress in x, y directions, u_b, v_b are the flow velocity near the bed in x, y directions, C_f is the bed friction coefficient, s, n are the local streamline coordinate q_{bx}, q_{by} are the bedload flux in x, y directions, u_{px}, u_{py} are the bedload particle velocity in x, y directions, q_{be} is the equilibrium bedload flux, τ_* is the Shields number, τ_{*c} is the critical Shields number, l_s is the step length, L_a is the active layer thickness, S_g is the specific weight of sediment in fluid, μ_c is the dynamic Coulomb friction coefficient, B is the model constant proposed by Madsen and Sorensen (1992) .

Results

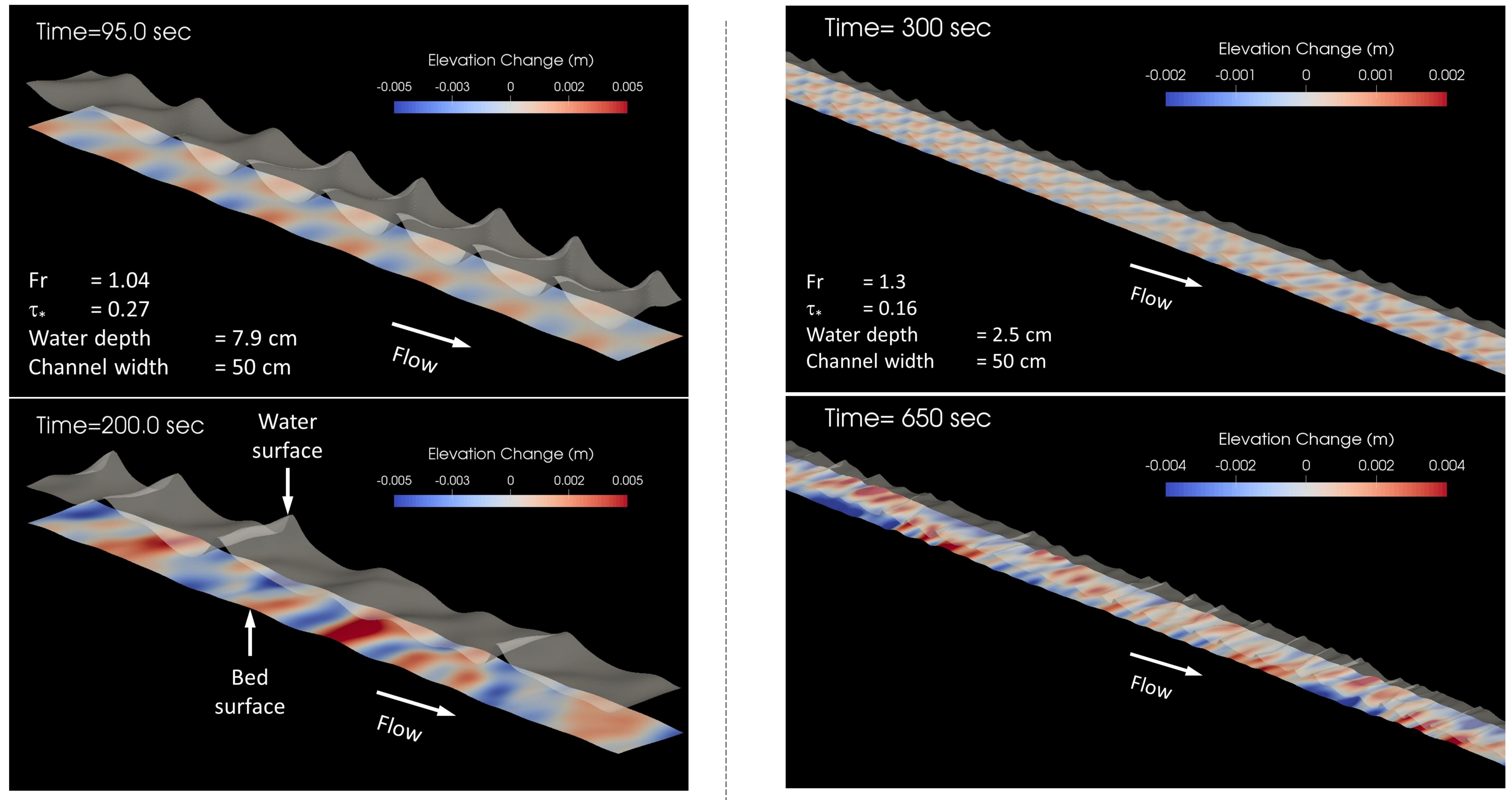

Figure 4. Numerical results of the 3D antidune and water surface wave dynamics. Left) relatively narrow channel (Channel width/depth = 6.3, Fr = 1.04, τ_* = 0.27), and right) relatively wide channel (Channel width/depth = 20, Fr = 1.3, τ_* = 0.16)

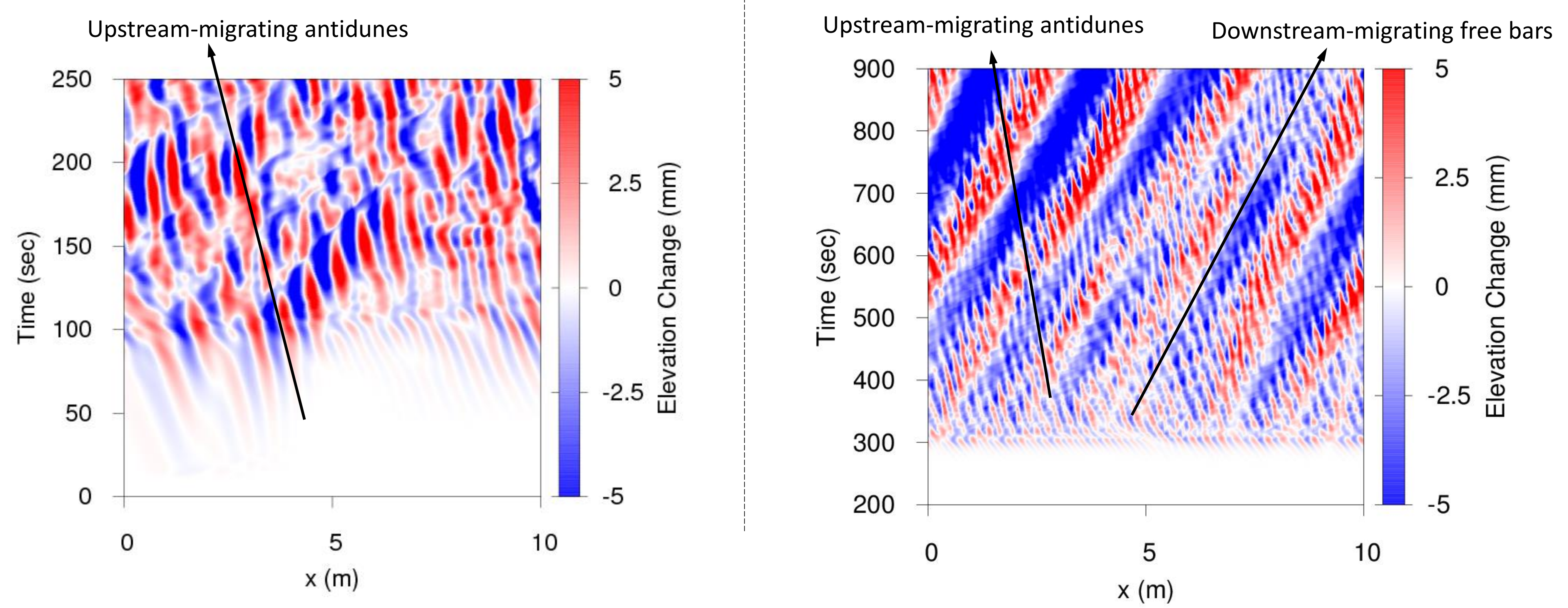

Figure 5. Time series of the bed elevation change from the initial bed near the right bank given from the simulated bed bathymetry (Figure 4).

- ✓ The model simulates three-dimensional antidunes (Upper panel of Figure 4). The left figure of Fig. 4 shows an antidune like an alternate bar, but the wavelength is much shorter than the bar scale. Right figure of Fig. 4 shows the formation of multiple antidunes in transverse direction. These antidunes mostly migrate upstream (Figure 5).
- ✓ The long time calculation somewhat changes the initially-formed antidunes as shown in bottom panel of Figure 4. The simulated antidunes tend to be 2D antidunes (left figure of Fig. 4), and in relatively wide channel for which the alternate bar can form, the upstream-migrating antidune coexists with downstream-migrating free bars.

Conclusion

- ✓ We proposed a depth-integrated model to capture three-dimensional antidunes. The model performance is investigated by fully-nonlinear numerical simulations.
- ✓ The model can reproduce the formation and development of three-dimensional antidunes, and also coexistence of antidune and free bars.
- ✓ The limitations of the model are 1) simulated 3D antidunes tend to lose their three-dimensionality, and 2) the model can not reproduce downstream-migrating antidunes.

References
Iwasaki et al., 2016, AGU2016.
Madsen and Sorensen, 1992, Coastal Engineering